

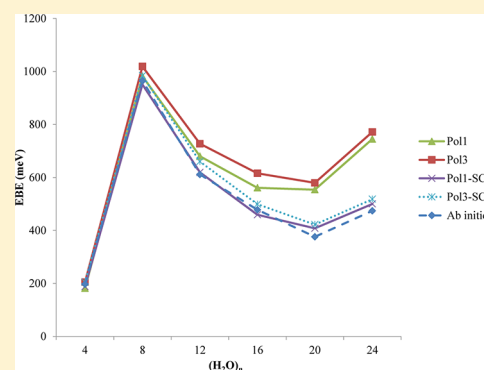
# A Self-Consistent Polarization Potential Model for Describing Excess Electrons Interacting with Water Clusters

Vamsee K. Voora,<sup>†</sup> Jing Ding,<sup>†</sup> Thomas Sommerfeld,<sup>‡</sup> and Kenneth D. Jordan<sup>\*,†</sup>

<sup>†</sup>Department of Chemistry and Center for Molecular and Materials Simulations, University of Pittsburgh, Pittsburgh, Pennsylvania 15260, United States

<sup>‡</sup>Department of Chemistry and Physics, Southeastern Louisiana University, Hammond, Louisiana 70402, United States

**ABSTRACT:** A new polarization model potential for describing the interaction of an excess electron with water clusters is presented. This model, which allows for self-consistent electron–water and water–water polarization, including dispersion interactions between the excess electron and the water monomers, gives electron binding energies in excellent agreement with high-level ab initio calculations for both surface-bound and cavity-bound states of  $(\text{H}_2\text{O})_n^-$  clusters. By contrast, model potentials that do not allow for a self-consistent treatment of electron–water and water–water polarization are less successful at predicting the relative stability of surface-bound and cavity-bound excess electron states.



## 1. INTRODUCTION

The nature of excess electrons in bulk water, at water interfaces, and attached to water clusters continues to be a topic of considerable debate.<sup>1–7</sup> Computer simulations using one-electron model potentials have played an important role in elucidating the structure and dynamics of an excess electron in water systems.<sup>1,2,8–16</sup> However, the usefulness of such simulations is directly related to the quality of the electron–water and water–water models employed. One of the most intriguing aspects of these systems is the importance of long-range dispersion-type interactions between the excess electron and the electrons of the water molecules.<sup>17</sup> As a result, excess electron–water systems are also valuable for exploring the use of model potential approaches for describing long-range electron correlation effects.

Over the past several years, our group has introduced two one-electron model Hamiltonian approaches for treating negatively charged water clusters.<sup>8,18</sup> The first approach describes the dynamical response of the electrons of the water monomers to the excess electron by means of quantum Drude oscillators.<sup>18</sup> The simultaneous excitation of the excess electron and of a Drude oscillator describes the dispersion interaction between the excess electron and a water monomer. The second approach models the dynamical response of water molecules to the excess electron by means of a polarization potential. As shown in ref 8, a polarization potential model can be derived from the Drude model by adiabatic separation of the excess electron and the Drude oscillator degrees of freedom.

In general, our Drude and polarization model approaches give similar electron-binding energies, but for some water clusters, in particular, larger clusters with interior bound excess electrons, there are sizable differences in the electron binding

energies (EBEs) calculated using the two approaches.<sup>8</sup> It is not known whether this is due to an inherent limitation of the polarization model or due to differences in the parametrization of the two approaches. Moreover, for these problem cases, both model potential approaches give EBEs that differ appreciably from the results of high-level electronic structure calculations.<sup>19</sup>

A major approximation of both our Drude model and polarization model approaches is the neglect of coupling of the electron–water and water–water polarization. The importance of such self-consistency has been noted by Jacobsen and Herbert<sup>1</sup> and by Stampfli.<sup>16</sup> In the present paper, we introduce a polarization model in which these coupled polarization interactions are treated self-consistently. The performance of the new model, referred to as Pol3-SC, is assessed by comparing the resulting EBEs with the results of accurate ab initio calculations for clusters as large as  $(\text{H}_2\text{O})_{24}^-$ .<sup>19</sup> It is found that treating electron–water and water–water polarization self-consistently is especially important for the cavity-bound anions of the larger clusters.

The Pol3-SC model introduced in the present study shares several features with the recently introduced electron–water model of Jacobson et al.<sup>15</sup> In particular, both approaches are based on a water model with distributed mutually interacting dipole polarizable sites, although there are differences in the water–water force-fields used (the AMOEBA force-field<sup>20</sup> by Jacobson et al. and the distributed point polarizable (DPP)

**Special Issue:** Paul F. Barbara Memorial Issue

**Received:** July 12, 2012

**Revised:** September 13, 2012

**Published:** September 19, 2012

force-field<sup>21</sup> in our work). Both models use a spatial grid for solving the energy of the one-electron Hamiltonian. However, while Jacobson et al. solve for the electron–water polarization using the entire spatial distribution of the excess electron, we use an adiabatic approach in which the induced dipoles on the waters adjust to the position of the electron instantaneously. As a result, our model accounts for long-range correlation interactions between the excess electron and the electrons of the water molecules, while such correlation effects are not recovered in the self-consistent field (SCF)-type treatment of Jacobsen and Herbert. In this regard, our model is actually closer in spirit to that of Stampfli.<sup>16</sup> Two major differences between our approach and Stampfli's are the use of three polarizable sites on the monomer in our model versus one in Stampfli's model, and the parametrization of our model to accurate ab initio EBEs.

## 2. THEORETICAL DETAILS

**2.1. Description of the Present Drude and Polarization Model Approaches.** Both model potential approaches developed in our group have been designed to work with the polarizable DPP water model,<sup>21</sup> which employs three point charges, positive charges on the H atoms, and a balancing negative charge at the so-called *M* site, located on the rotational axis and displaced 0.25 Å from the O atom toward the H atoms. In addition, the DPP model employs three mutually interacting atom-centered point polarizable sites with Thole-damping<sup>22</sup> of the charge-induced dipole and induced-dipole–induced-dipole interactions. Exchange-repulsion is represented by exponentials between all atoms of different molecules, and dispersion interactions are represented as damped  $C_6/R^6$  contributions between the O atoms. The resulting one-electron Hamiltonian, in atomic units, is of the form

$$\hat{H}^{\text{el}} = -\frac{1}{2}\nabla^2 + V^{\text{es}} + V^{\text{rep}} + V^{\text{e,ind}} + V^{\text{dr}} \quad (1)$$

where  $V^{\text{es}}$  accounts for the electrostatic interaction between the excess electron and the charges of the monomers,  $V^{\text{rep}}$  represents the short-range repulsion between the monomers and the excess electron,  $V^{\text{e,ind}}$  couples the excess electron to the induced dipoles from water–water polarization, and  $V^{\text{dr}}$  represents the dynamic response of water monomers to the excess electron.  $V^{\text{dr}}$  is described by either Drude oscillators or polarization potentials. Because there is no coupling between the last two terms in eq 1, these models neglect changes in the water–water interactions resulting from the dynamical response of the water monomers to the excess electron.

In our applications of the Drude oscillator approach, we employed a single Drude oscillator per water monomer located at the *M*-site, giving a coupling term of the form

$$V^{\text{dr}} = \sum_o \frac{Q\mathbf{R}_{\text{oe}} \cdot \mathbf{R}_o^{\text{D}}}{(R_{\text{oe}})^3} f(R_{\text{oe}}) \quad (2)$$

where  $\mathbf{R}_{\text{oe}}$  determines the position of the electron relative to the oscillator,  $\mathbf{R}_o^{\text{D}}$  determines the location of the displaceable fictitious charge  $-Q$ , with respect to a countering fictitious charge  $+Q$  fixed at the *o* site, and  $f(R_{\text{oe}})$  is a damping function that attenuates the unphysical behavior as  $R_{\text{oe}}$  goes to zero.

The parameters in the Drude model consist of  $b$ , which controls the damping of  $V^{\text{dr}}$  by  $f$  and  $\gamma$  that scales the repulsive potential, as well as the force constant  $k$ , mass  $m_{\text{D}}$ , and the fictitious charge  $Q$  associated with the Drude oscillator. The

polarizability of the Drude oscillator  $\alpha_{\text{D}}$  is given by  $Q^2/k$  and is taken to be equal to the experimental value of the isotropic polarizability of water. In our applications of the method,  $Q$  has been taken to be +1, which fixes the value of  $k$ . With these assumptions, the excitation energy of the Drude oscillator,  $\epsilon_{\text{D}}$  is 8.7 eV, a reasonable value for the mean excitation energy of a water monomer. A perturbative analysis shows that the classical polarization contribution of the excess electron–water interaction depends on  $Q^2/k$  but not on  $\epsilon_{\text{D}}$ .<sup>18</sup> However, the dispersion energy in the Drude model depends on both  $Q^2/k$  and  $\epsilon_{\text{D}}$ , which means that it acquires a dependence on  $m_{\text{D}}$ . The EBEs calculated with the Drude model, at least for the small  $(\text{H}_2\text{O})_n^-$  clusters, tend to be relatively insensitive to the choice of  $m_{\text{D}}$ , and in our applications of this approach, we have used  $m_{\text{D}} = m_{\text{e}}$ .

In most polarization model approaches, the interaction potential between the excess electron and a polarizable site *i* is described by a term of the form

$$V^{\text{dr}}(R_{ie}) = -\frac{\alpha_i}{2R_{ie}^4} g(R_{ie}) \quad (3)$$

where,  $\alpha_i$  is the dipole-polarizability of the *i*th site, and  $g(R_{ie})$  is a damping function to remove the divergence as  $R_{ie}$  tend to zero. An alternative to the use of a damping function is the inclusion of a shift parameter in the denominator.

In ref 8 it was shown that the interaction of an electron with a single Drude oscillator gives rise to an adiabatic potential of the form

$$V_{\text{ad}}(r) = \epsilon_{\text{D}} - \sqrt{\epsilon_{\text{D}}^2 + \frac{\epsilon_{\text{D}}\alpha_{\text{D}}}{r^4} f^2(r)} \quad (4)$$

where  $f(r)$  is the damping function used in the Drude model. Thus it is seen that the adiabatic potential depends on both  $Q^2/k$  and  $\epsilon_{\text{D}}$ , which for a fixed  $k$  value means that it depends on  $m_{\text{D}}$ . A Taylor series expansion of this potential, retaining only up to the leading term in  $\alpha_{\text{D}}$ , gives the traditional polarization potential of eq 3.

**2.2. Pol3-SC Model.** As noted above, the quantum Drude and polarization models introduced by our group in the past do not treat the water–water and electron–water polarization self-consistently. This limitation is removed in the Pol3-SC model in which the potential for electron–water interaction,  $\hat{V}^{\text{e-w}}$ , consists of electrostatic, repulsion, and self-consistent polarization terms:

$$\begin{aligned} \hat{V}^{\text{e-w}} = & -\sum_i \frac{q_i}{R_{ie}} f_{\text{pc}}(R_{ie}) + \sum_i V_i^{\text{rep}}(R_{ie}) \\ & - \frac{1}{2} \sum_{ij} (V_{ij}^{\text{e-w,pol}}(\mathbf{R}_{ie}, \mathbf{R}_{ij}) - V_{ij}^{\text{w-w,pol}}(\mathbf{R}_{ij})) \end{aligned} \quad (5)$$

where the first term on the right-hand side represents the electrostatic interactions between the electron and the charge sites on the monomers, the second term represents the short-range repulsive interactions between the electron and atomic sites, and the third term is the electron–water self-consistent polarization potential, which is described in detail below.  $f_{\text{pc}}$  damps the electrostatic interaction at short-range and is necessitated by the use of a discrete variable representation (DVR) basis set.<sup>23</sup> The repulsive potential associated with each monomer was determined using the procedure described in ref

18 and is represented in terms of four *s*-type Slater functions on each atom:

$$V_i^{\text{rep}} = \sum_{k=1}^4 a_k e^{-\xi_k R_{ie}} \quad (6)$$

In our earlier work a Gaussian-type basis set was employed to describe the wave function of the excess electron and the repulsive potential was represented in terms of Gaussian functions to facilitate evaluation of the resulting integrals. In the present work, a DVR grid basis set is employed, with the consequence that it is advantageous to use a Slater function representation of the repulsive potential.

Because the DPP water model employs three polarizable sites per monomer, the implementation of a fully self-consistent treatment of the electron–water and water–water polarization necessitates the use of three polarizable sites per water for describing electron–water polarization. This is in contrast to our earlier polarization model, which employed a single polarizable site per monomer for describing electron–water polarization. The short-range divergence of the electron–water polarization interaction is avoided by replacing  $R_{ie}$  with  $R_{\text{eff}}(R_{ie})$  where, the effective distance,  $R_{\text{eff}}$  is defined as

$$R_{\text{eff}}(R) = \begin{cases} R, & \text{if } R \geq d; \\ d \left( \frac{1}{2} + \left( \frac{R}{d} \right)^3 \left( 1 - \frac{R}{2d} \right) \right), & \text{if } R < d \end{cases} \quad (7)$$

The net polarization potential is

$$\begin{aligned} \frac{1}{2} \sum_{ij} V_{ij}^{\text{e-w,pol}}(\mathbf{R}_{ie}, \mathbf{R}_{ij}) \\ = \frac{1}{2} \sum_{ij} (\mathbf{E}_i^{\text{e}}(\mathbf{R}_{ie}) + \mathbf{E}_i^{\text{w}}(\mathbf{R}_i)) \cdot (\alpha_{ii}^{-1} - \mathbf{T}_{ij}^{(2)}(\mathbf{R}_{ij}))^{-1} \cdot (\mathbf{E}_j^{\text{e}}(\mathbf{R}_{ie}) + \mathbf{E}_j^{\text{w}}(\mathbf{R}_j)) \end{aligned} \quad (8)$$

where,  $\mathbf{E}_i^{\text{w}}$  is the static electric field at site *i* due to the charge sites of the other water molecules, and  $\mathbf{E}_i^{\text{e}}$  is the electric field on the atomic site *i* due to the excess electron.  $\mathbf{R}_{ij} = \mathbf{R}_j - \mathbf{R}_i$  is the distance vector between sites *i* and *j*,  $\alpha_{ii}$  is a matrix of the site polarizabilities, and  $\mathbf{T}_{ij}^{(2)}$  is the interaction matrix between induced dipoles on sites *i* and *j*. In the absence of the electron, eq 8 reduces to the polarization potential for water–water interactions,  $V^{\text{w-w,pol}}$ , which, of course, does not contribute to the EBE and is already included in the water force-field. The polarization potential for the excess electron is given by the difference between  $V^{\text{e-w,pol}}$  and  $V^{\text{w-w,pol}}$ . In the absence of the interaction between induced dipoles on different water molecules (i.e.,  $\mathbf{T}_{ij} = 0$ ), the inverse matrix in eq 8 becomes diagonal, and the polarization potential reduces to

$$\frac{1}{2} \sum_i V_{\text{e-w}}^{\text{pol}}(\mathbf{R}_{ie}) = \frac{1}{2} \sum_i \mathbf{E}_i^{\text{e}} \cdot \alpha_i \cdot \mathbf{E}_i^{\text{e}} = \frac{1}{2} \sum_i \frac{\alpha_i}{(R_{\text{eff}}(R_{ie}))^4} \quad (9)$$

Therefore, one can view the electron–water polarization term as having three contributions: interaction of the electron with the induced dipoles from water–water interactions, polarization of the water monomers by the excess electron, and the cross terms that allows the water–water interaction to adjust to the electron–water interactions.

In addition to the Pol3-SC model, we report results for three other models, designated Pol1, Pol3, and Pol1-SC. Pol1 uses a single polarizable site per monomer and Pol3 three polarizable sites per monomer for treating the electron–water interactions. Neither of these models allows for a self-consistent treatment of electron–water and water–water polarization. The Pol1-SC model, like Pol3-SC, treats electron–water and water–water polarization self-consistently but uses only a single polarizable site per monomer for describing electron–water monomer polarization. Pol1, Pol3, and Pol1-SC use the same parametrization procedure as Pol3-SC to facilitate comparison of results obtained using the various methods.

**2.3. Parameterization of the Model Potentials.** The model potentials contain three parameters: the scaling parameter  $\gamma$  for the repulsive potential, the parameter *d* in the electron–water polarization potential, and a damping parameter in the electrostatic interaction between the excess electron and water molecules. The calculated EBEs are relatively insensitive to the choice of the electrostatic damping parameter, which is arbitrarily chosen to be equal to  $\sqrt{\pi}$ . The scaling parameter for the repulsive potential was chosen so that for the W6a hexamer anion (see Figure 1), the model potential using point charges chosen to reproduce the Hartree–Fock value of the dipole of the monomer and without the electron–water polarization gives the same EBE as obtained from a large basis set Hartree–Fock calculation on the neutral cluster using

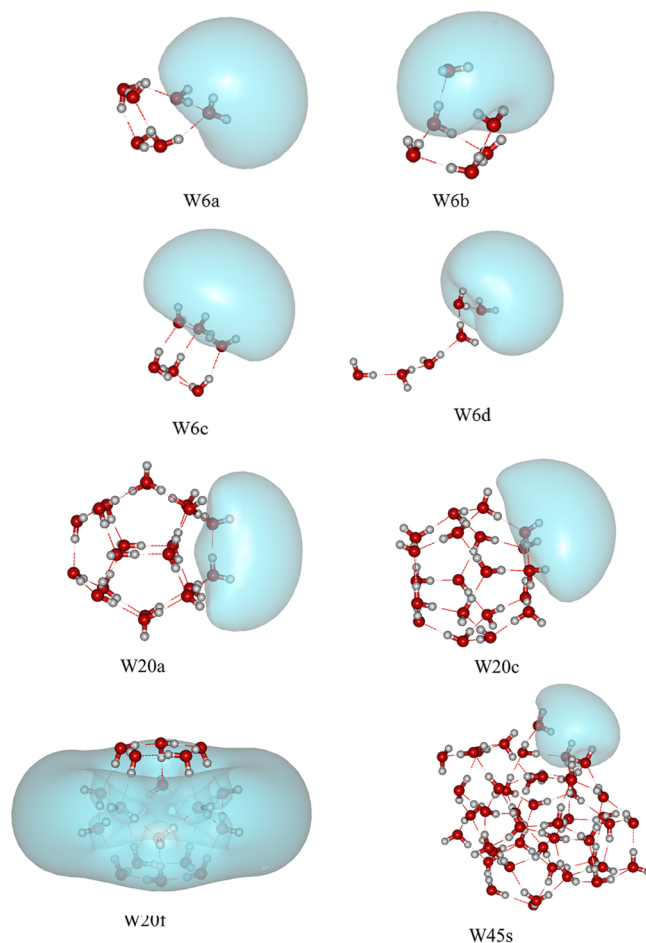


**Figure 1.** Water clusters with a surface bound excess electron. The charge densities of the excess electrons are depicted using a surface that encloses 90% of the charge.



the Koopmans' theorem<sup>24</sup> approximation. The  $d$  parameter in the electron–water polarization potential was chosen such that the EBE of W6a from the model potential approach using point charges that reproduce the CCSD dipole moment of water monomer is the same as that obtained from large basis set CCSD(T)<sup>25</sup> calculations.

In the implementation of the new polarization models in our PISCES code,<sup>26</sup> we employ sine-type particle-in-the-box functions within a DVR approach.<sup>23,27</sup> The results reported in this study were obtained using an evenly spaced  $80 \times 80 \times 80$  cubic DVR grid with 80 Bohrs sides, which is adequate to achieve well converged energies.

**2.4. Testing of the Polarization Models for EBE.** A series of water clusters ranging from the hexamer to selected  $(\text{H}_2\text{O})_{24}^-$  isomers was used to test the Pol3-SC and simpler models. The geometries of the clusters were taken from our earlier studies,<sup>8,19</sup> and, in each case, employed rigid monomers. The ab initio methods used to benchmark the EBEs include the second-order algebraic diagrammatic correction [ADC(2)] method,<sup>28</sup> and second-order and coupled-cluster singles-doubles equation-of-motion methods, designated EOM-MP2<sup>29,30</sup> and EOM-CCSD,<sup>31</sup> respectively. We have recently shown that these three approaches generally give similar values of the EBEs of  $(\text{H}_2\text{O})_n^-$  clusters,<sup>19</sup> and for several of the clusters, we use the ab initio results from this earlier study. The test systems include six isomers of  $(\text{H}_2\text{O})_6^-$ , labeled W6a–W6f, a  $(\text{H}_2\text{O})_8^-$  cluster designated W8a, three  $(\text{H}_2\text{O})_{20}^-$  clusters, designated W20a, W20c, W20e, two  $(\text{H}_2\text{O})_{24}^-$  clusters denoted W24a and W24c, and W4, W8, W12, W16, and W20 subclusters extracted from W24a. For the  $(\text{H}_2\text{O})_6^-$ ,  $(\text{H}_2\text{O})_{20}^-$ , and  $(\text{H}_2\text{O})_{24}^-$  clusters, the nomenclature scheme of ref 8 is adopted. The cluster structures are shown in Figures 1 and 2. W6a–W6d, W20a, W20c, and W45s all have sizable dipole moments and surface bound anions. W20f is an example of a cluster with no net dipole, but with a surface-bound anion. The remaining clusters are models for interior (i.e., cavity bound) excess electron states. W6f has the classic Kevan type structure,<sup>32</sup> and W8a has a closely related structure. W24a has been generated by adjusting the structure of the W24a considered previously so that the overall symmetry is  $D_{2h}$  and the monomers have the gas-phase structure.

### 3. RESULTS AND DISCUSSION

Tables 1 and 2 report the EBEs obtained with the four models and from ab initio calculations when available. From the results reported in Table 1, it is seen that for the clusters with surface-bound excess electrons, the different model potential approaches give nearly the same value of the EBE. Moreover, for the subset of these clusters for which high-level ab initio results are available, the model potential and ab initio EBEs are in excellent agreement. By contrast, with the exception of W4 and W6e, for the larger clusters with cavity-bound anions, the self-consistent Pol3-SC model gives EBEs appreciably smaller than those obtained from the Pol-1 model, with the differences being 227, 270, and 451 meV for W24a, W24c, and W45i, respectively. Most importantly, the Pol3-SC EBEs are in very good agreement with the ab initio results when available.

For W12, W16, W20, and W24a, the Pol3-SC calculated EBEs are 21–49 meV larger than the ab initio results. However, for these cases, much of the discrepancy is likely due to non-completely converged ab initio values rather than to limitations in the Pol3-SC model. The nonconvergence of the ab initio EBEs comes from two sources: (1) the use of the ADC(2)

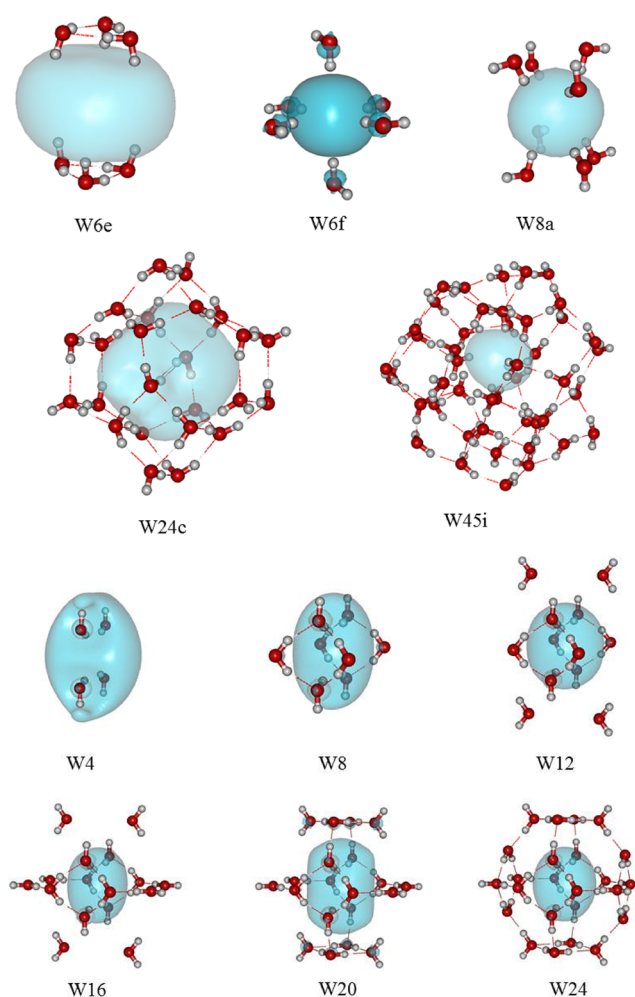


**Figure 2.** Water clusters with interior-bound excess electron. W4 has significant surface-bound character but is included here as it is derived from W24a. The charge densities of the excess electrons are depicted using a surface that encloses 90% of the charge.

**Table 1.** EBEs (in meV) of Surface Bound Excess Electron States of  $(\text{H}_2\text{O})_n^-$  Clusters

cluster	EBE				
	ab initio <sup>a</sup>	Pol1	Pol3	Pol1-SC	Pol3-SC
W6a	429	423	422	425	423
W6b	572	569	567	559	559
W6c	330	346	338	344	338
W6d	349	331	328	339	336
W20a		1047	1039	1036	1029
W20c		656	650	646	644
W20f		354	347	332	327
W45s		1474	1469	1403	1394

<sup>a</sup>EBEs calculated using the EOM-MP2 method and the aug-cc-pVTZ basis set<sup>33,34</sup> augmented with a set of diffuse 6s, 6p, and 6d functions at the center of mass.

method rather than the computationally more demanding EOM-CCSD method for the larger clusters, and (2) the truncation of the atomic basis sets. On the basis of exploratory EOM-CCSD calculation on W16, it appears that the converged EBEs of the W12, W16, W20, and W24a model clusters could be 20–80 meV greater than the ADC(2) ab initio values reported in ref 19. For W6a, the cluster used for the

**Table 2.** EBEs (in meV) of Internal Excess Electron States of  $(\text{H}_2\text{O})_n^-$  Clusters

cluster	ebe				
	ab initio	Pol1	Pol3	Pol1-SC	Pol3-SC
W6e	533 <sup>a</sup>	563	560	540	541
W6f	823 <sup>b</sup>	801	903	764	831
W8a	965 <sup>a</sup>	984	1160	880	992
W4	197 <sup>b</sup>	182	205	188	205
W8	965 <sup>b</sup>	982	1018	951	984
W12	611 <sup>b</sup>	680	727	619	660
W16	478 <sup>b</sup>	561	616	459	499
W20	376 <sup>b</sup>	554	579	408	422
W24a	474 <sup>b</sup>	745	772	500	518
W24c		468	434	237	198
W45i		2500	2540	2038	2049

<sup>a</sup>From EOM-MP2 calculations using the aug-cc-pVTZ basis set augmented with a 7s7p set of diffuse functions located at the center of mass. <sup>b</sup>From ref 19. Results for W4 and W8f are from EOM-MP2 calculations. The results for W6f and W12–W24a are from ADC(2) calculations.

parametrization, the model potential EBEs are slightly (4–7 meV) smaller than the ab initio result reported in Table 1. This is simply a consequence of our repeating the ab initio calculations with a larger basis set after the model potentials were parametrized.

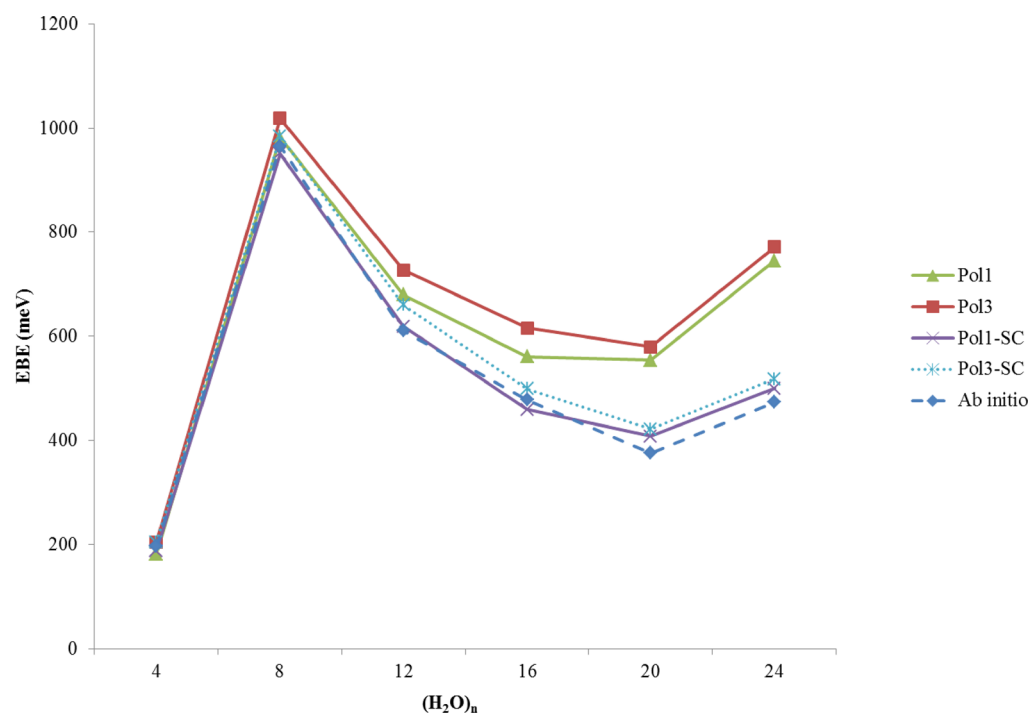
It was noted above that the four model potential approaches introduced in this study give similar EBEs for the surface-bound anions. A very different situation is found for the interior-bound excess electron species. For W8 and W12–24a, the models that treat electron–water and water–water polarization self-consistently give much smaller EBEs than do the models that do not. Surprisingly, with the exception of W6f and W8a, the use of three polarizable sites per monomer proves relatively unimportant. For W6f and W8a, the models with three

polarizable sites give appreciably larger EBEs than those employing a single polarizable site. However, the reduction in the EBE upon inclusion of self-consistent electron–water and water–water polarization is more important when the model includes three polarizable sites, with the result that the Pol1 model fortuitously gives EBEs similar to those from the Pol3-SC model and from ab initio calculations for W6f and W8a. For the larger clusters, the coupling of the electron–water and water–water polarization proves more important with the result that the Pol3-SC model gives significantly smaller EBEs than obtained with the Pol1 model.

Figure 3 reports the EBEs of the subclusters of W24a as described by the Pol1, Pol3, Pol1-SC, and Pol3-SC models and the corresponding ab initio results from ref 19. This figure clearly demonstrates the growing importance of many-body electron–water polarization effects with increasing cluster size. This is readily understood by the unfavorable orientation of the induced dipoles on the different water monomers resulting from the polarization of the monomers by the excess electron. Allowing for interaction between the induced dipoles results in a weakening of the EBE.

All model potential results discussed to this point were obtained by parametrizing the calculated EBE to W6a, which has a surface-bound excess electron state. We also parametrized the four models to W8a in which the excess electron is largely cavity-bound. With this parametrization, the errors in the nonself-consistent models are roughly halved for the cavity-bound excess electron states, while there is only minor degradation of the results for surface-bound anions. This appears to be the consequence of the parametrization to W8a resulting in a weaker electron–water repulsive potential, which, in turn, leads to more strongly damped electron–water polarization interactions.

We have also tested the various models on the calculation of the electronic excitation energies of the clusters. As expected,

**Figure 3.** Variation in EBE upon progressive build-up of the W24a cluster. Ab initio results are from ref 19.

the energies of the *p*-like excited states are less impacted by the self-consistent treatment of electron–water and water–water polarization than are the ground state energies. For the W45i cluster, the Pol3-SC model gives an excitation energy of 1.66 eV versus the 1.93 eV value obtained with the Pol1 model.

#### 4. CONCLUSIONS

In this work we introduced a self-consistent polarization model for the interaction of an excess electron with water clusters. The present study and those of Jacobson et al.<sup>1</sup> and of Stampfli<sup>16</sup> demonstrate that a self-consistent treatment of electron–water and water–water polarization is important for establishing the relative energies of the surface-bound and cavity-bound excess electron species. For a representative W45 cluster, the self-consistent treatment of electron–water interactions changes the relative stability of surface-bound and cavity-bound anions by as much as 320 meV. In that context, it is interesting to note that much of the recent computational work on excess electron–solvent systems has used a non-self-consistent treatment of electron–solvent and solvent–solvent interactions.<sup>2,8,35,36</sup> Most encouragingly, the present work and that of ref 15 indicate that carefully parametrized self-consistent polarization models can account in a quantitative manner for the binding of excess electrons to water clusters.

One disadvantage of polarization model approaches is that they do not allow one to separate the many-body effects into dispersion, induction, and induction–dispersion contributions. To accomplish this separation, it would be highly desirable to extend the Drude model described in the Introduction to account for many-body interactions involving the excess electron and two or more Drude oscillators. Efforts along this line are underway in our group.

#### AUTHOR INFORMATION

##### Corresponding Author

\*E-mail: jordan@pitt.edu.

##### Notes

The authors declare no competing financial interest.

#### ACKNOWLEDGMENTS

This research was carried out with the support of the National Science Foundation under NSF grant CHE1111235.

#### REFERENCES

- (1) Jacobson, L. D.; Herbert, J. M. *Science* **2011**, 331, 1387.
- (2) Turi, L.; Sheu, W.-S.; Rossky, P. J. *Science* **2005**, 309, 914–917.
- (3) Larsen, R. E.; Glover, W. J.; Schwartz, B. J. *Science* **2010**, 329, 65–69.
- (4) Bragg, A. E.; Verlet, J. R. R.; Kammrath, A.; Cheshnovsky, O.; Neumark, D. M. *J. Am. Chem. Soc.* **2005**, 127, 15283–15295.
- (5) Siefermann, K. R.; Liu, Y.; Lugovoy, E.; Link, O.; Faubel, M.; Buck, U.; Winter, B.; Abel, B. *Nat. Chem.* **2010**, 2, 274–279.
- (6) Ben-Amotz, D. *J. Phys. Chem. Lett.* **2011**, 2, 1216–1222.
- (7) Hammer, N. I.; Roscioli, J. R.; Bopp, J. C.; Headrick, J. M.; Johnson, M. A. *J. Chem. Phys.* **2005**, 123, 244311.
- (8) Sommerfeld, T.; DeFusco, A.; Jordan, K. D. *J. Phys. Chem. A* **2008**, 112, 11021–11035.
- (9) Choi, T. H.; Jordan, K. D. *Chem. Phys. Lett.* **2009**, 475, 293–297.
- (10) Sommerfeld, T.; Jordan, K. D. *J. Phys. Chem. A* **2005**, 109, 11531–11538 PMID: 16354045.
- (11) Turi, L.; Borgis, D. J. *Chem. Phys.* **2002**, 117, 6186–6195.
- (12) Barnett, R. N.; Landman, U.; Cleveland, C. L.; Jortner, J. *Phys. Rev. Lett.* **1987**, 59, 811–814.

- (13) Barnett, R. N.; Landman, U.; Cleveland, C. L.; Jortner, J. *J. Chem. Phys.* **1988**, 88, 4429–4447.
- (14) Schnitker, J.; Rossky, P. J. *J. Chem. Phys.* **1987**, 86, 3462–3470.
- (15) Jacobson, L. D.; Williams, C. F.; Herbert, J. M. *J. Chem. Phys.* **2009**, 130, 124115.
- (16) Stampfli, P. *Phys. Rep.* **1995**, 255, 1–77.
- (17) Gutowski, M.; Skurski, P.; Boldyrev, A. I.; Simons, J.; Jordan, K. D. *Phys. Rev. A* **1996**, 54, 1906–1909.
- (18) Wang, F.; Jordan, K. D. *J. Chem. Phys.* **2002**, 116, 6973–6981.
- (19) Vysotskiy, V. P.; Cederbaum, L. S.; Sommerfeld, T.; Voora, V. K.; Jordan, K. D. *J. Chem. Theory Comput.* **2012**, 8, 893–900.
- (20) Ren, P.; Ponder, J. W. *J. Phys. Chem. B* **2003**, 107, 5933–5947.
- (21) Defusco, A.; Schofield, D. P.; Jordan, K. D. *Mol. Phys.* **2007**, 105, 2681–2696.
- (22) Thole, B. *Chem. Phys.* **1981**, 59, 341–350.
- (23) Light, J. C.; Carrington, T. *Adv. Chem. Phys.*; John Wiley and Sons, Inc.: New York, 2007; pp 263–310.
- (24) Koopmans, T. *Physica* **1934**, 1, 104–113.
- (25) Raghavachari, K.; Trucks, G. W.; Pople, J. A.; Head-Gordon, M. *Chem. Phys. Lett.* **1989**, 157, 479–483.
- (26) Sommerfeld, T.; Choi, T.-H.; Voora, V. K.; Jordan, K. D. Unpublished results.
- (27) Choi, T. H.; Sommerfeld, T.; Yilmaz, S. L.; Jordan, K. D. *J. Chem. Theory Comput.* **2010**, 6, 2388–2394.
- (28) Schirmer, J.; Cederbaum, L. S.; Walter, O. *Phys. Rev. A* **1983**, 28, 1237–1259.
- (29) Nooijen, M.; Snijders, J. G. *J. Chem. Phys.* **1995**, 102, 1681–1688.
- (30) Stanton, J. F.; Gauss, J. *J. Chem. Phys.* **1995**, 103, 1064–1076.
- (31) Nooijen, M.; Bartlett, R. J. *J. Chem. Phys.* **1995**, 102, 3629–3647.
- (32) Feng, D.-F.; Kevan, L. *Chem. Rev.* **1980**, 80, 1–20.
- (33) Dunning, T. H., Jr. *J. Chem. Phys.* **1989**, 90, 1007–1023.
- (34) Kendall, R. A.; Dunning, T. H., Jr.; Harrison, R. J. *J. Chem. Phys.* **1992**, 96, 6796–6806.
- (35) Mones, L.; Turi, L. *J. Chem. Phys.* **2010**, 132, 154507.
- (36) Mones, L.; Rossky, P. J.; Turi, L. *J. Chem. Phys.* **2011**, 135, 084501.